Association for Information and Image Management
1100 Wayne Avenue, Suite 1100
Silver Spring, Maryland 20910
301/587-8202

Centimeter

Inches

MANUFACTURED TO AIIM STANDARDS
BY APPLIED IMAGE, INC.

1 of 1

CONF-940812--9
SAND94-1532C

NAK POOL-BOILER BENCH-SCALE RECEIVER DURABILITY TEST: TEST RESULTS AND MATERIALS ANALYSIS

Charles E. Andraka, Steven H. Goods, Robert W. Bradshaw,
James B. Moreno, Timothy A. Moss, Scott A. Jones

IECEC94-3865

SAND94-1532C

Sandia National Laboratories
Albuquerque, New Mexico 87185

ABSTRACT

Pool-boiler reflux receivers have been considered as an alternative to heat pipes for the input of concentrated solar energy to Stirling-cycle engines in dish-Stirling electric generation systems. Pool boilers offer simplicity in design and fabrication. The operation of a full-scale pool-boiler receiver has been demonstrated for short periods of time. However, to generate cost-effective electricity, the receiver must operate without significant maintenance for the entire system life, as much as 20 to 30 years.

Long-term liquid-metal boiling stability and materials compatibility with refluxing NaK-78 is not known and must be determined for the pool boiler receiver. No boiling system has been demonstrated for a significant duration with the current porous boiling enhancement surface and materials. At least one theory explaining incipient-boiling behavior of alkali metals indicates that favorable start-up behavior should deteriorate over time. Many factors affect the stability and startup behavior of the boiling system. Therefore, it is necessary to simulate the full-scale pool boiler design as much as possible, including flux levels, materials, and operating cycles. On-sun testing is impractical because of the limited test time available.

A test vessel was constructed with a Friction Coatings Inc. porous boiling enhancement surface. The boiling surface consisted of a brazed stainless steel powder with about 50% porosity. The vessel was heated with a quartz lamp array providing about 90 W/cm² peak incident thermal flux. The vessel was charged with NaK-78, which is liquid at room temperature. This allows the elimination of costly electric preheating, both on this test and on full-scale receivers. The vessel was fabricated from Haynes 230 alloy, selected for its high temperature strength and oxidation resistance. The vessel operated at 750°C around the clock, with a 1/2-hour shutdown cycle to ambient every 8 hours. Temperature data was continually collected.

The test completed 7500 hours of lamp-on operation time, and over 1000 startups from ambient. The test was terminated when a small leak in an Inconel 600 thermowell was detected. The test design and data are presented here. Metallurgical analysis of virgin and tested materials has begun, and initial results are also presented.

This work performed by Sandia National Laboratories supported by the U.S. Department of Energy under contract DE-AC04-94AL85000. This paper is declared a work of the U.S. Government and is not subject to copyright protection in the United States.

BACKGROUND

Sandia National Laboratories (SNL), together with the U.S. Department of Energy (DOE), has identified dish-Stirling electric systems as having potential to meet the DOE Solar Thermal Energy Program's long-term goals for levelized energy cost [1,2]. SNL is cooperating with industry to develop and commercialize dish-Stirling systems. Several of these systems have proposed the use of reflux receivers. The liquid-metal reflux receiver was conceived of as an improvement over directly illuminated tube receivers [3,4]. In the reflux receiver approach, liquid metal is evaporated at the solar absorber and condensed at the engine heater tubes, supplying the latent heat of vaporization to the engine. The liquid at the absorber may be a pool that floods the surface (pool boiler) or a wick saturated with liquid metal that covers the absorber surface (heat pipe). The operation and advantages of reflux receivers have been well documented [5].

The feasibility of the pool-boiler receiver approach was demonstrated in 1989-1990 [6]. The demonstration receiver achieved power throughputs exceeding 60 kW_t at efficiencies of about 90%. Based on these results, a second-generation pool-boiler receiver was designed [7]. A series of short-term bench-scale receiver tests was performed to qualify the materials and methods applied to the new receiver [8]. Based on these results and ease of manufacture, a Friction Coatings Inc. powdered-metal surface was selected for the boiling enhancement surface. In addition, a small amount (1/3 torr) of xenon was added to the NaK vapor space to promote stable boiling and smooth startups. This amount was based on previous on-sun tests as well as extensive bench-scale testing [6,8]. The second-generation receiver incorporates materials and methods proposed for long-life, commercial devices and demonstrated in the series of bench-scale tests. The shell material is Haynes 230, a high strength nickel-based alloy. The receiver was designed to ASME Boiler and Pressure Vessel Code intent and was manufactured and inspected using techniques typical in small production volumes. The receiver was filled with NaK-78, a liquid at room temperatures, eliminating the need for electric pre-heaters. The second-generation receiver was successfully tested on sun [9,10].

DISTRIBUTION OF THIS DOCUMENT IS UNLIMITED

MASTER

Thermacore Inc. demonstrated stable boiling in a bench scale of a similar sintered surface over a period of about 800 hours [11]. The boiling behavior did not appear to change during this test period. Other short-term boiling studies [12] have shown a change in boiling characteristics due to the reduction of oxides on the boiling surface. Once the oxides are reduced, the liquid metal wets the surface and quenches the nucleation sites, causing high incipient-boiling superheats. The porous powdered metal surfaces used in the Thermacore and present tests contain a large surface area protected by tortuous paths, and therefore may take a considerable period of time to be fully reduced and wetted. However, dish-Stirling systems have an expected life of 20 to 30 years, about 60,000 hours of solar-only operation. Nucleate boiling also induces small temperature fluctuations at the nucleation site at the bubble departure frequency [13], which could possibly lead to thermal fatigue failure of the enhanced surface. In addition, the Haynes 230 alloy and the braze materials in the Friction Coatings surface have not been qualified for operation in alkali metals at high temperature. Since it would be very difficult to put a meaningful number of hours on a full-scale test, we planned a 10,000-hour, around-the-clock, bench-scale test with the selected materials and methods. The duration of the test was selected because it is a significant fraction of the required life, is attainable in a little over 1 year, and is more than an order of magnitude longer than previous experiments.

TEST DESIGN

The test vessel was designed to be heated with a six-bulb quartz lamp array, simulating the fluxes experienced in a full-scale on-sun test. The peak flux at full power is about 90W/cm² with a total power throughput of 1500W_t. The test specimen is a 1-3/4-inch-diameter, Haynes 230 alloy, welded tube with brazed-on endcaps. The tube wall thickness is 0.049 inches. Figure 1 shows a schematic of the test. The tube is 2 feet long, arranged vertically, and filled to about 10.75 inches with NaK-78 (approximately 0.75 pounds). The tube is shorter than previous bench-scale tests in order to promote mixing of splashed liquid with the xenon, which tends to be swept to the top end of the pipe. The entrainment of xenon to the pool is thought to assist in hot restarts and boiling stability [8]. In as many areas as possible, the parameters of this test were designed to simulate the full-scale test[14]. The enhanced boiling surface is a 1 x 4-inch patch of porous 304 Stainless steel. The patch was fabricated from -60/+80 non-spherical powder by Friction Coatings Inc. The surface has an estimated effective pore radius of 50 μm and an estimated void fraction of 50%. The patch covered the high flux portion of the heated area and was 0.030-inches thick. A strip of zirconium foil, 1-inch by 12-inches, was placed in the bottom of the test vessel to hot-getter any oxygen present in the NaK-78. Instrumentation consisted primarily of type-K thermocouples brazed to the surface or inserted in Inconel 600 alloy thermowells.

Power extraction from the condenser is primarily by passive radiation to the room. The power throughput estimates are based on prior operation of the same test vessel with the same lamp array but with a gas-gap, cold-water calorimeter to measure power extraction [8]. Enough insulation was removed from the condenser (top end) of the device to maintain the setpoint temperature with one of the six heater-array bulbs failed. In addition, a small muffin fan was activated when all lamps are on and the test vessel was at temperature. A PID control loop determines the lamp operating voltage based on the pool temperature. During startup, the lamp power ramps from 0 to 100% power in less than 3 seconds, simulating a full-power on-sun startup.

Temperature and pressure data were recorded at 1 second intervals during transients and 5 second intervals during steady operation. Details of the test setup can be found in references 14 and 15.

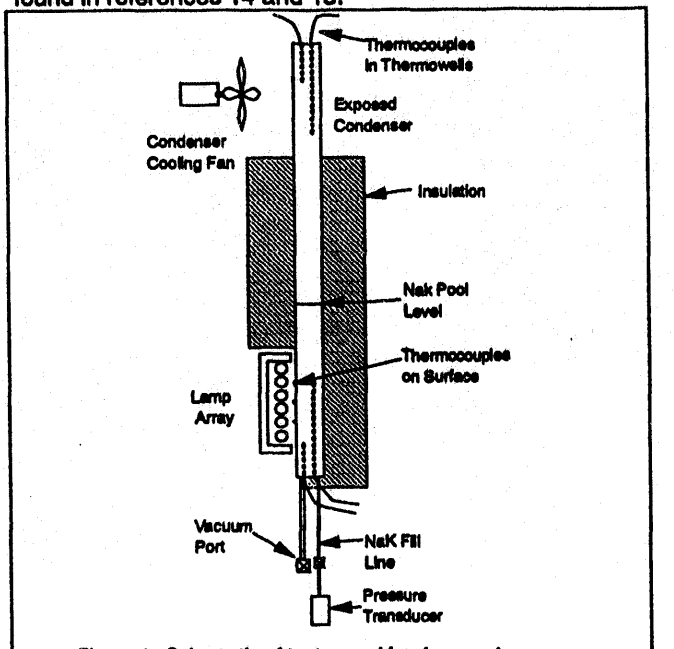

Figure 1. Schematic of test vessel hardware setup

INITIAL TEST RESULTS

To simulate the diurnal solar cycle, the test was designed to automatically cycle to "ambient" temperatures every 8 hours. After extended operation at temperature, pre-existing metal oxides on the enhanced boiling surface may be reduced, allowing the NaK to wet the surface. The cycle to ambient stops vapor formation and allows the NaK to fully penetrate the clean nucleation sites. Changes in the startup behavior would indicate that oxide reduction affects the boiling process. The cycles also subject the surface to the low-cycle thermal fatigue associated with frequent startups. The cool-off period is set at 30 minutes, which results in a restart temperature under 150°C. The normal temperature setpoint is 750°C pool temperature. During a cold restart, full lamp power is applied with the condenser cooling fan turned off. As the setpoint temperature is approached, the PID controller reduces the lamp power to about 83% and the condenser fan is turned on, if all six bulbs are still functional. The system takes approximately 6.5 minutes to reach the setpoint temperature under normal conditions. The reduced power at steady state results in a peak flux of 76 W/cm² and a power throughput of about 1170 W. Cloud transients are not simulated in this study.

Figure 2 shows a typical day in the life of the pool boiler, with three 7.5-hour operations at temperature. The temperature traces of the pool, vapor, and surface ther-

mocouples demonstrate the steady nature of the boiling. Approximately a 5°C temperature drop is seen from the pool to the condenser. The surface thermocouples are in the peak flux region, so they read slightly higher than the actual surface temperature. The "noise" on the pressure signal is actually the result of pressure waves from the boiling. During the 30-minute shutdowns, the indicated pressure is steady.

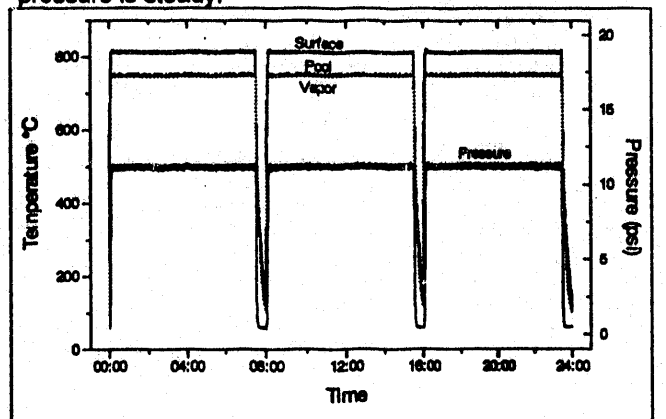

Figure 2. A day in the life of the durability-pool-boiler test. Every 8 hours the test is cycled to "ambient" temperatures to simulate the diurnal solar cycle. The pool and vapor temperatures are about 5 degrees apart.

The test device operated for about 7500 hours of lamp-on time with over 1000 cold startups. There was no detectable change in the system behavior during steady state operation or startups. Figure 3 shows cold startups at midnight on a weekly basis. No significant difference is seen between the different traces. Several spikes are seen in the surface and pool temperatures at startup. The temperature spikes do not appear to be increasing in frequency or severity as test time progresses and have not been seen in the on-sun tests of full-scale receivers. The spread in the curves is primarily due to changes in the ambient temperature and minor adjustments of test setup.

The large amount of data generated, over 600 Mb, is difficult to evaluate. The daily data was reduced to an average and standard deviation of each measured variable over a span of 1000 readings (5000 seconds) after steady state operation was reached. Days with multiple heater lamp bulb failures, when the pool operating temperature could not maintain 750°C, were rejected. Figure 4 shows this data summary.

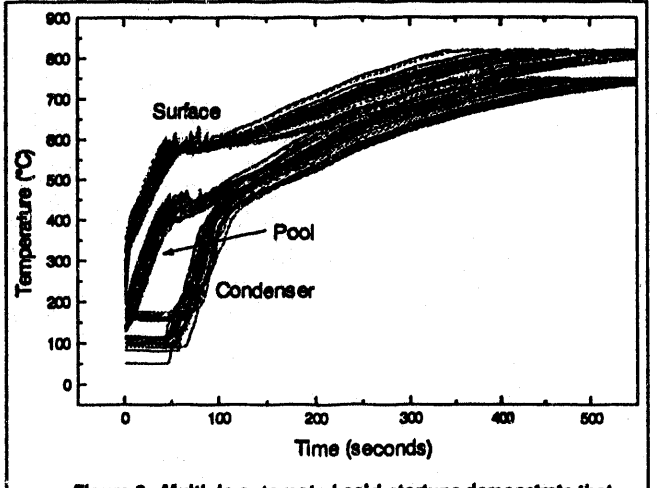

Figure 3. Multiple automated cold startups demonstrate that the startup behavior does not change with time. This plot includes a weekly sample cold startup for the duration of the test.

A small amount of relative drift is seen in the internal thermocouples but is within the thermocouple accuracy. More importantly, the standard deviation of the front-surface thermocouples does not change over the duration of the test, indicating that steady boiling behavior is unchanged. In mid-April, the lamp cooling system was modified and the condenser thermocouple replaced, resulting in a step change in the temperature difference from the pool to the condenser. In late August, the device could not maintain the pool temperature, possibly because of settling insulation. The condenser area was slightly reduced to compensate, and this also resulted in a step-change in the temperature difference. However, the temperature difference does not change appreciably over the life of the test, indicating there was no significant increase in the internal non-condensable gas pressure.

On January 5th, the boiler was operating at lower-than-usual power, and the temperature difference between the pool and condenser had increased, indicating the presence of gas in the pipe. We observed a small amount of green crust at the top of the condenser thermowell, indicating a leak in the vessel. The pressure gauge indicated a cold pressure of about .75 psia, compared to a normal reading of about .55 psia. The data indicated that the leak occurred within the previous 24 hours.

We decided to drain the boiler and distill out the residual NaK. Distillation produces a very clean specimen, avoiding the caustic products associated with steam or alcohol cleaning. However, distillation requires that the leak be stopped using a patch with high-temperature capability. We used a small closed-end stainless-steel cylinder welded over the area where the thermowell emerged from the boiler. Welding was chosen in order to obtain the required high-temperature capability. Torch brazing was rejected because of its larger heat-affected zone and

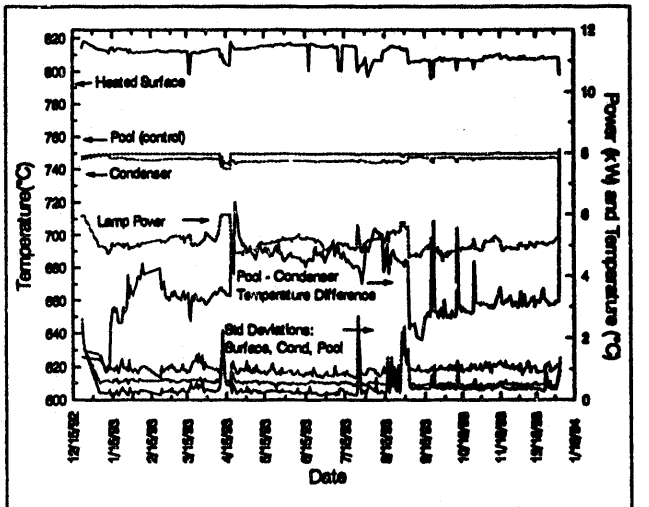

Figure 4. Summary of steady-state data. The average and standard deviation of 1000 readings each day on select instruments are presented here. No significant increase in temperature fluctuations (standard deviation) or temperature difference is seen throughout the test.

The tendency of braze-filler alloys to spread. Such effects might have obscured the cause of the leak.

METALLURGICAL ANALYSIS

A detailed metallurgical analysis of the materials used in the construction of the bench-scale durability-test pool boiler is underway. The results presented below are preliminary and are primarily related to liquid-metal corrosion. We shall report results at a later date [16] that address the full range of our concerns, which includes:

1. Liquid-metal and air-side corrosion of the boiler materials.
2. Boiling-related thermal or mechanical fatigue of the powder-metal coating.
3. Deleterious microstructural changes in the boiler materials and joints.
4. Loss of strength or ductility of the boiler materials.

Our approach consists of the following steps:

1. Analysis preliminaries:
   a. Pre-test archiving of as-delivered materials and assemblies for comparison with the tested boiler.
   b. Post-test patching of the boiler leak.
   c. Draining and distillation-cleaning of the boiler under vacuum.
   d. Archiving of the NaK.
2. Analysis:
   a. Pool-boiler dissection and microscopy.
   b. Elemental analysis of NaK and NaK- and air-exposed surfaces.
   c. Measurement of pool-boiler vessel mechanical properties

Analysis preliminaries

The archived, as-delivered materials were drawn from the same material lots used to construct the tested boiler. The archive includes Haynes Alloy 230 1.75-inch tubing, samples of the Friction Coating Inc. powder-metal coating, a duplicate of one end of the boiler (including samples of all the tubing, weldments, and braze joints), a sample of zirconium (hot getter) sheet stock, and the high-purity NaK-78 in its original shipping container.

The boiler was connected to a vacuum manifold that included a 900-cc steel can to receive the used NaK. The manifold and can were evacuated and the boiler was drained into the can through a 150-mesh screen filter. The boiler and manifold were purged with argon, evacuated to about 3×10^{-3} torr, and then heated to 450°C. After one week, the temperatures were allowed to return to ambient. The patch over the leak was removed by machining without disturbing the thermowell. The boiler was cut in half and the valves were cut off with tubing cutters. A small amount of NaK was found in the valves, but the boiler appeared to be NaK-free and clean (Figure 5 and Figure 6). The getter disintegrated into a number of small pieces (Figure 7). Bubble testing located the leak near the closed end of the thermowell, just above the braze joint connecting it to the condenser wall. A photograph of this area appears in Figure 8.

Analysis

As mentioned earlier, the analysis presented here is primarily concerned with liquid-metal induced corrosion. Corrosion by liquid metals can manifest itself in a number of ways. Dissolution of alloying or interstitial (e.g. carbon) elements is the simplest of these corrosion mechanisms as it results directly from the solubility of various elements in the molten metal. Alternately, reactions between alloy constituents and impurities in the molten metal (such as oxygen) are often important. In this case, reaction products that may or may not be soluble in the molten metal can be formed. In the present test, a zirconium-metal oxygen getter was employed, and we expect that corrosion of the containment materials by residual oxygen in the NaK was minimal.

Figure 5. Condenser end of dissected pool boiler, showing free-standing vapor-temperature thermowells and wall-temperature thermowells brazed to the condenser wall. The longer of the two wall-temperature thermowells is the one that leaked.

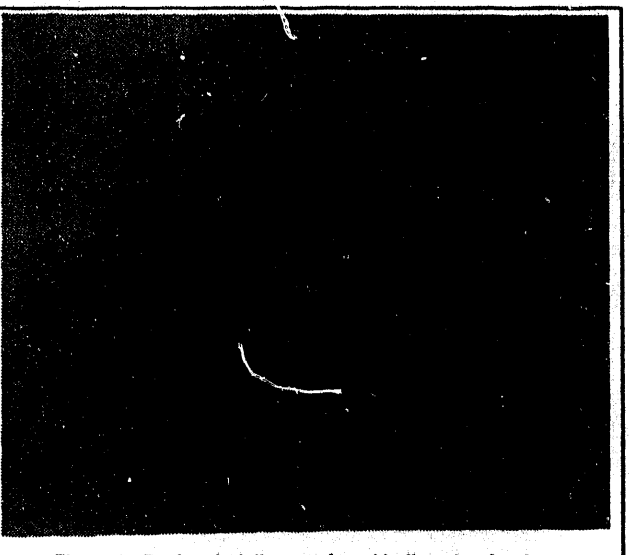

Figure 6. Pool end of dissected pool boiler, showing free-standing pool-temperature thermowells and powder-metal coating on the heated surface.

Preliminary results of a metallurgical analysis of the response of the pool boiler materials is presented below. Materials exposed to both the NaK pool and NaK vapor condensate are being examined as is the NaK itself.

Haynes 230 alloy – As-received

The pool-boiler vessel is constructed of Haynes 230, a high performance alloy used primarily for elevated-temperature applications in hostile environments. Haynes

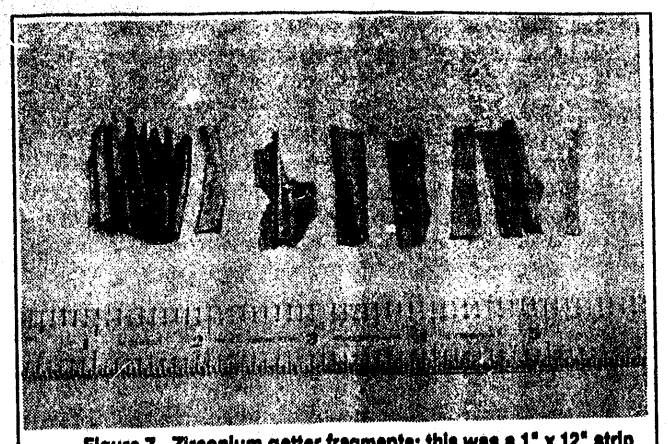

Figure 7. Zirconium getter fragments; this was a 1" x 12" strip that was corrugated and rolled into a cylinder shape, and fitted into the bottom of the boiler.

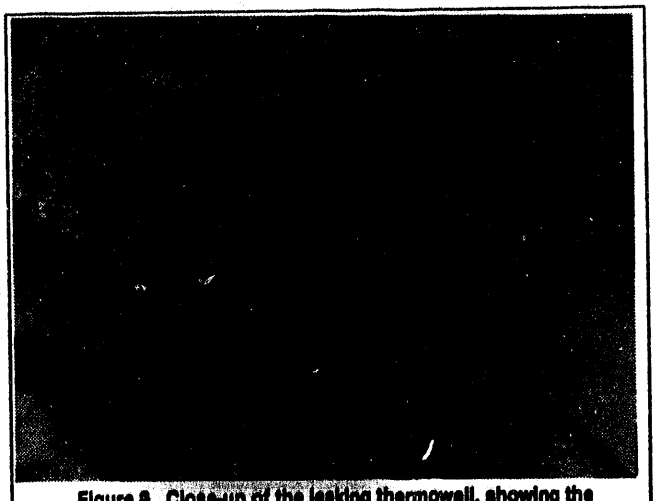

Figure 8. Close-up of the leaking thermowell, showing the necked area caused by cyclic thermal strain, where the leak occurred.

230 is a nickel-chromium-tungsten-molybdenum alloy that contains small additions of iron, cobalt, silicon and aluminum. It has good microstructural stability and exhibits excellent strength retention and resistance to grain growth after prolonged high-temperature exposure. Table I shows the alloy specification and the heat analysis of the 1.75-inch-diameter seam-welded tubing.

For the current application, autogenously-welded tubing was supplied in the solution-heat-treated condition. This heat treatment was performed in vacuum at 1175-1245°C (as specified by Haynes). The Rockwell hardness of the alloy after heat treating was Rb 94. A second-phase microstructure remains even after solution heat treatment. A scanning electron micrograph of the as-received alloy (polished cross section), shown in Figure 9, reveals that the material contained a relatively uniform distribution of second-phase particles.

Energy dispersive spectroscopy (EDS), a semi-quantitative technique, was used to characterize the composition of the alloy and its microstructure. The overall composition of the alloy obtained from an area scan of the as-received tubing is shown in Table I. The results agree favorably with the heat analysis supplied with the tubing. Also shown in Table I is a spot-mode

TABLE I: Elemental analyses of HAYNES 230 (by EDS), wt%

LOCATION	Ni	Cr	W	Fe	Mo	Co
Specification	bal	20-24	13-15	3 †	1-3	5 †
Heat analysis	bal	21.96	14.06	1.45	1.26	0.29
As-received (area)	66.75	19.99	10.43	1.01	1.28	0.39
2nd phase* (spot)	28.82	15.45	47.73	0.76	6.59	0.00
Region a	42.71	9.49	41.97	1.66	3.76	0.00
Region b	64.61	19.03	12.87	2.40	1.10	0.00

*As-received
†max
Haynes 230 is a tradename of Haynes International, Inc., Kokomo, IN.

analysis of a second phase particle that indicates the precipitates have an elevated tungsten concentration.

Figure 10 is a scanning electron micrograph of the ID of the as-received tubing. Marks from the tube forming process are evident in the micrograph. EDS analysis indicates that the particulates on the surface have the same composition as that indicated in Table I for the second phase.

Pool-boiler sidewall -- exposed to NaK pool

Scanning electron micrographs of the inside of the Haynes 230 pool boiler exposed to the 750°C NaK pool are shown in Figure 11a,b. Figure 11a, a low magnifica-

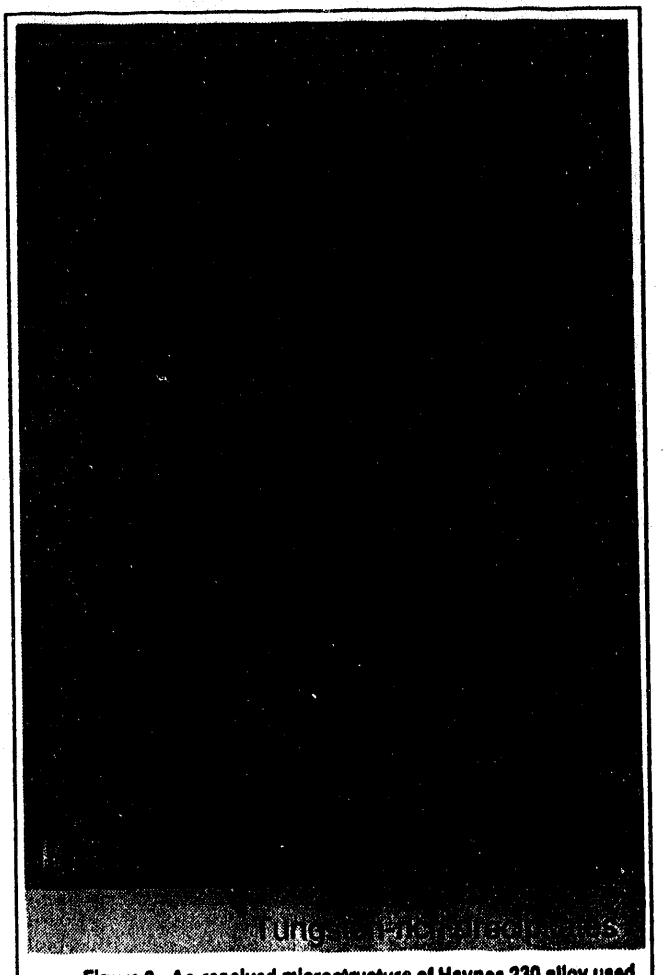

Figure 9. As-received microstructure of Haynes 230 alloy used in construction of pool boiler. Solution heat-treated alloy contains a uniform distribution of tungsten-rich precipitates.

tion image of the alloy surface, reveals a complex structure clearly altered from the as-received tubing. At higher magnification, Figure 11b reveals that the structure consists of particulates uniformly decorating the surface. EDS analysis has been used to characterize the composition of these features and the base material. These results are also shown in Table I. The particulates (indicated in the Table as REGION A) have a composition similar to the second phase particles identified in the previous section. The prominence of the precipitates in Figure 11b results from the recession of the matrix.

Reliable solubility data for the transition metals and tungsten in liquid NaK are quite limited. However, nickel and chromium are known to have solubilities of several parts per million in liquid sodium [17], so the recession of the alloy surface can be attributed to the dissolution of nickel and chromium in the liquid metal pool. A spot analysis of the alloy surface between the precipitates (REGION B) is given in Table I and reveals that the NaK-pool-exposed alloy matrix maintains the composition of the as-received alloy. Grain boundaries can be seen beneath the precipitate structure in Figure 11b suggesting that dissolution of the alloy is more rapid at the grain boundaries than within the grains. Such grain boundary "grooving" is another common feature of liquid metal interactions with metals and alloys. Initial metallographic cross-sections prepared from samples exposed to the NaK pool indicate that the amount of recession is only a few microns (we used the tungsten-rich particulates as markers for the original surface). If this recession were uniform over the interior of the boiler, it would amount to about 0.25 cm^3 or 2 grams of material. We have not yet been able to account for this material by analysis of the NaK or by locating re-deposited alloy constituents on the internal surfaces of the boiler.

Examination of the surface morphology of the autogenous seam weld exposed to the NaK pool indicates that there were no significant differences from the wrought alloy surface just described. The recession of the alloy matrix and the degree to which the tungsten-rich precipitates decorate the surface in the weld zone are both comparable to that shown in Figure 11a,b for the parent metal.

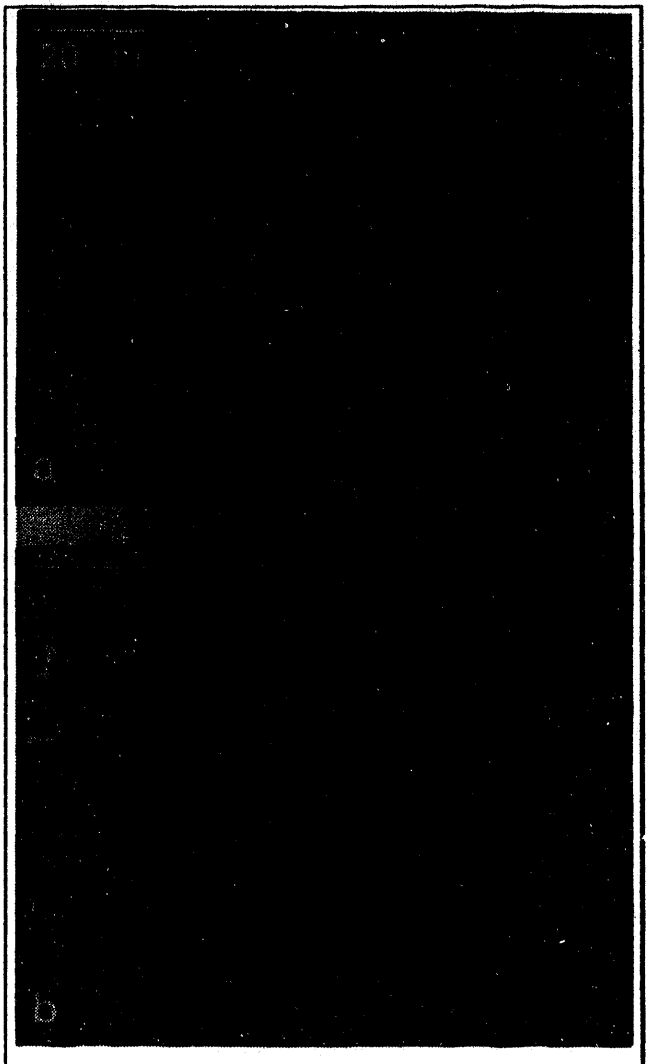

Figure 10. a) Internal surface of as-received Haynes 230 tubing; b) Higher-magnification image reveals presence of W-rich precipitates at the tube surface.

Pool boiler sidewall — exposed to NaK condensate

Above the pool surface, the boiler sidewall is exposed to NaK condensate as well as to liquid ejected from the pool. The condensate will be relatively pure (free from metallic solutes). It will also be relatively rich in po-

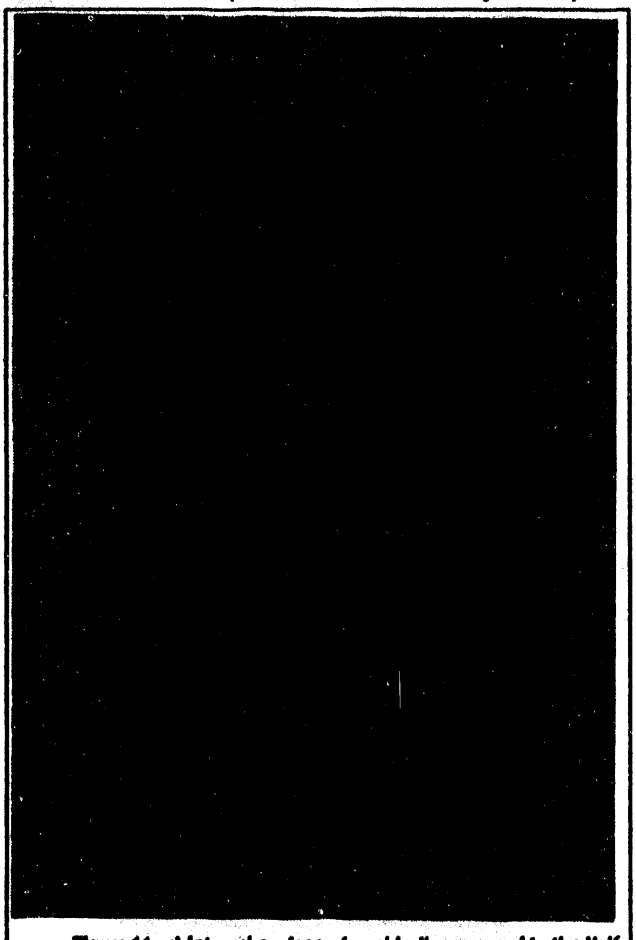

Figure 11. a) Internal surface of pool-boiler exposed to the NaK pool for 7500 hours. Features on the surface are precipitates exposed by the recession of the alloy matrix; b) Higher magnification reveals the morphology of the surface structure and the presence of grain boundary dissolution. Regions A and B refer to locations of EDS analysis in Table I.

tassium, because the vapor pressure of potassium is much higher than the vapor pressure of sodium. As a result, the extent of dissolution of alloy constituents from the pool-boiler sidewall may depend on whether the location is above or below the pool surface.

Visual examination of the pool boiler revealed a distinct "waterline" delineating the surface exposed to the NaK pool from the surface in the condensing region. Figure 12 shows the structure of the sidewall of the vessel in the condenser region. The surface has a morphology intermediate between the as-received material and the NaK-pool-exposed surface. The tungsten-rich precipitates are less well defined than those shown in the previous figures, suggesting that the degree of dissolution of the matrix is somewhat less extensive. However, the grain boundary grooving is more apparent than before simply because the precipitate structure is less well defined and does not mask the grain boundary structure. The composition of both the precipitates and of the underlying matrix are essentially identical to that reported for the surface exposed to the NaK pool.

As before, the seam weld appears to have been affected to the same extent as the parent alloy. Lastly, the Rockwell hardness of the vessel was Rb 92 suggesting that there were no changes in the mechanical properties of the material as a result of the long-term exposure to NaK or the prolonged time at temperature. Strength and ductility of the pool-boiler vessels will be directly measured as part of this metallurgical analysis and reported later [16].

Powder-metal coating on heated surface

The heated surface was coated with Type 304L stainless-steel -60/+80 powder adhered to the surface with a braze filler alloy equivalent to Bni-7, a nickel-chromium-phosphorous alloy. A visual inspection of the coating (Figure 6) shows it to be entirely intact and free of any macroscopic cracking. This is an important preliminary result, because of ongoing concerns regarding thermal and mechanical fatigue effects of the liquid-metal bubble cycle. A detailed metallurgical analysis of the heated surface and its coating is in progress.

Inconel 600 thermowell

Inconel 600 (IN600) 1/8th-inch tubing was used to fabricate the six thermowells in the pool-boiler vessel. These thermowells were located above and below the NaK pool. IN600 is a nickel-chromium-iron austenitic alloy that has good resistance to oxidation and stress-corrosion cracking. However, there appears to be little published information regarding its resistance to liquid-metal attack. The specified composition for the alloy is given in Table II. At temperatures between 550 and 950°C, chromium carbides precipitate out of solid solution and may sensitize the material to intergranular attack in aggressive media.

TABLE II: Composition of Inconel 600 (wt%)

IN 600	Ni	Cr	Si	Fe	Mn	Cu
Specification	72*	14-17	0.5†	6-10	1.0†	0.50†

*Ni +Co = 72 min.
†Max
Inconel 600 is a product of the Inco Alloys International, Inc., Huntington, WV

Figure 13 shows the surface of a thermowell from the evaporator end of the boiler. It is clear that the alloy has suffered extensive intergranular dissolution. Similar attack was apparent on the thermowells in the condenser. Although not shown here, these grain boundary features connect to an extensive network of subsurface grain boundary cracks. Indeed, it was a through-section crack in one of these thermowells that resulted in the air leak, causing the test to be terminated. Figure 8 shows the failed thermowell. The crack was located at the base of the necked region evident in the Figure. This thermowell was brazed to the sidewall of the pool boiler vessel and thus was rigidly constrained at both ends. The necking and the associated crack were the direct result of this constraint. Differences in both the thermal expansion coefficients and the heating rates of the thermowell and the pool-boiler vessel gave rise to thermo-mechanical fatigue. The combined effects of fatigue and the chemical attack of NaK on the alloy was responsible for the failure of the tube and the subsequent termination of the experiment.

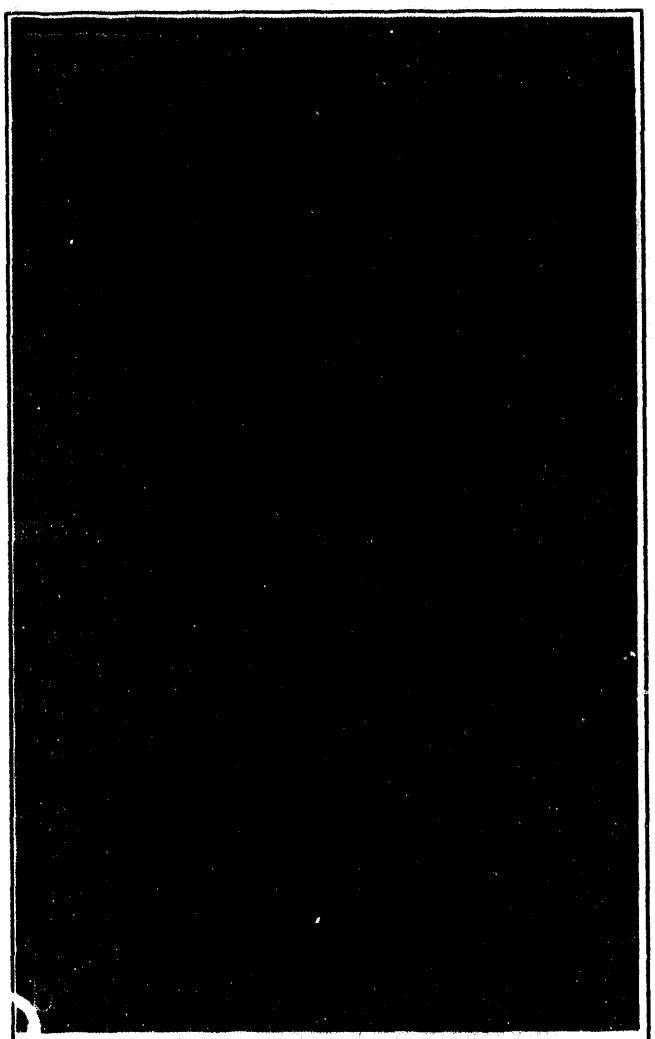

Figure 12. a) Internal surface of pool-boiler exposed to NaK condensate (above the pool). Precipitate structure is less well defined than in Figure 11 because of less-extensive alloy recession. Grain-boundary attack is more apparent; b) Higher magnification reveals the morphology of the surface structure.

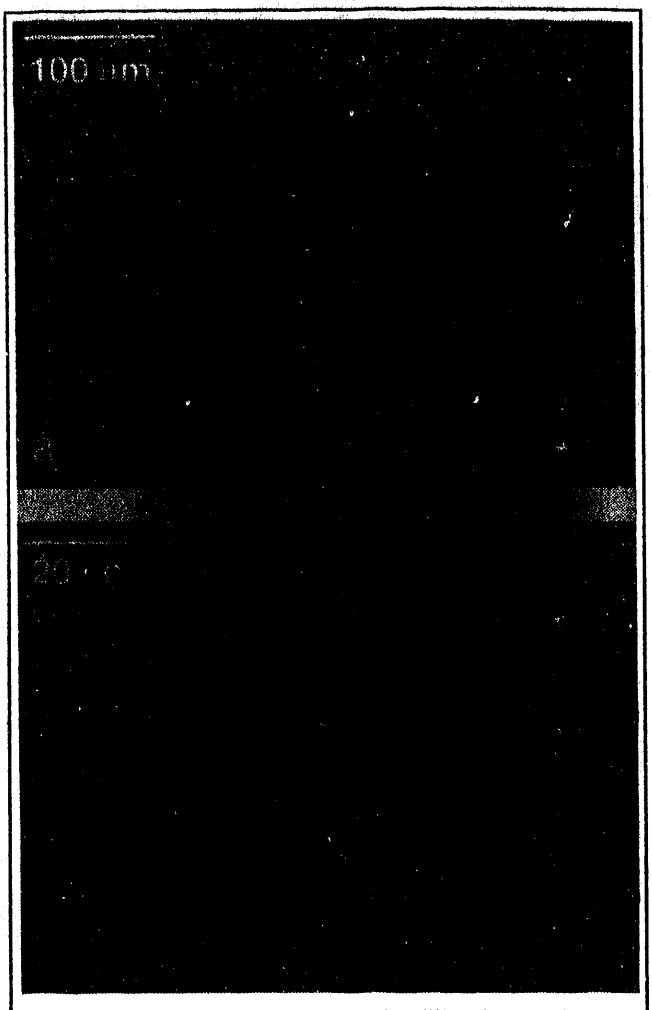

Figure 13. a) Grain-boundary attack of IN600 thermowell exposed to NaK pool; b) Surface and grain-boundary facetting of IN600 is apparent at high magnification.

CONCLUSIONS

1. A pool-boiler durability test operated for 7500 hours at 750°C with over 1000 cold startups. The operation and boiling behavior did not change during this period. The test simulated about 1/6 of the life expectancy of a full-scale solar pool boiler receiver using proposed full-scale materials and methods where possible.
2. The pool-boiler durability test was terminated after approximately 7500 hours due to a leak that developed in an IN600 thermowell. The leak was the result of intergranular dissolution and thermo-mechanical fatigue. It is emphasized that the use of IN600 in pool boiler designs is not essential. Even here, had the thermowell not been constrained at both ends, failure due to NaK interactions with IN600 would not have occurred until much later. Other alloys, more suitable for use in this application can be substituted in future experiments.
3. There was evidence of some interactions of Haynes 230 with the NaK environment. While the precise details of these interactions varied with location in the boiler, the minimal dissolution observed in the worst cases suggests that the alloy is suitable for use in further development studies and for longer periods of operation.
4. Hardness measurements suggest that there were no changes in mechanical properties of the Haynes 230. Direct measurement of residual mechanical properties are planned.
5. A preliminary examination of the powder-metal coating revealed no significant changes as a result of 7500 hours of operation.
6. Metallurgical analysis is continuing and a full detailed report is planned [16].

REFERENCES

1. Couch, W.A. ed., "Proceedings of the Annual Solar Thermal Technology Research and Development Conference," SAND89-0463, Sandia National Laboratories, Albuquerque, February, 1989.

2. Lukens, L.L., "Dish Electric Systems Heat Engine Assessment," SAND85-0522, Sandia National Laboratories, Albuquerque, June 1985.

3. "Solar Thermal Technology Annual Report, Fiscal Year 1986," prepared by Sandia National Laboratories and Solar Energy Research Institute, DOE/CH10093-12, July 1987.

4. Osborn, D. B. and Pons, R. L., "Solar Power Converter with Pool Boiling Receiver and Integral Heat Exchanger,", United States Patent 4,335,578, 1982.

5 Diver, R.B., et al, "Trends in Dish Stirling Solar Receiver Design," paper no. 905303, *Proceedings of the 25th IECEC*, Reno NV, August, 1990.

6. Andraka, C.E., et al, "Sodium Reflux Pool-Boiler Solar Receiver On-Sun Test Results," SAND89-2773, Sandia National Laboratories, Albuquerque, June 1992.

7. Moreno, J.B., et al, "Reflux Pool-Boiler as a Heat-Transport Device for Stirling Engines: Postmortem Analysis and Next-Generation Design," SAND91-11033C, Sandia National Laboratories, *Proceedings of the 26th IECEC*, August 1991.

8. Moreno, J.B., and T.A. Moss, "Bench Scale Screening Tests for a Boiling Sodium-Potassium Alloy Solar Receiver," SAND92-2253, Sandia National Laboratories, Albuquerque, 1993.

9. Moreno, J.B., et al, "First On-Sun Test of a NaK-78 Pool-Boiler Solar Receiver," SAND93-1207C, Sandia National Laboratories, *Proceedings of the 28th IECEC*, August 1993.

10 Moreno, J.B., et al, "On-Sun Test Results from Second-Generation and Advanced-Concepts Alkali-Metal Pool-Boiler Receivers," SAND93-1251, Sandia National Laboratories, Albuquerque, 1994.

11. Anderson, W.G, J.H. Rosenfeld, J. Noble, "Alkali Metal Pool Boiler Life Tests for a 25kW$_e$ Advanced Stirling Conversion System," *Proceedings of the 26th IECEC*, August 1991.

12. Singer, R.M., and R.E. Holtz, "The Vaporization of Superheated Sodium in a Vertical Channel," *Trans. ASME*, August 1972.

13. Shai, I., and W.M. Rohsenow, "The Mechanism and Stability Criterion for Nucleate Boiling of Sodium," *Trans. ASME, Series C, J. Heat Transfer*, 91:315 (1969)

14. Andraka, C.E., et al, "NaK Pool-Boiler Bench-Scale Receiver Durability Test: Test Design and Initial Results," SAND93-1208C, Sandia National Laboratories, *Proceedings of the 28th IECEC*, August 1993.

15. Andraka, C.E., et al, "NaK Pool Boiler Solar Receiver Durability Bench Test, Volume 1: Test Design and Results," SAND94-1538, Sandia National Laboratories, Albuquerque, to be published 1994.

16. Goods, S. H. , and Bradshaw, R. W., "NaK Pool Boiler Solar Receiver Durability Bench Test, Volume 2: Metallurgical Analysis", SAND94-8235, Sandia National Laboratories, Livermore, to be published 1994.

17. T. D. Claar, Reactor Tech., vol. 13, no. 2, p. 124 (1970).

DATE
FILMED
8/3/94

END